

## Temperature Dependence of the Kondo Resonance in $\text{YbAl}_3$

L. H. Tjeng,<sup>1,\*</sup> S.-J. Oh,<sup>2</sup> E.-J. Cho,<sup>2</sup> H.-J. Lin,<sup>1</sup> C. T. Chen,<sup>1</sup> G.-H. Gweon,<sup>3</sup> J.-H. Park,<sup>3</sup> J. W. Allen,<sup>3</sup>  
T. Suzuki,<sup>4</sup> M. S. Makivić,<sup>5</sup> and D. L. Cox<sup>5</sup>

<sup>1</sup>*AT&T Bell Laboratories, 600 Mountain Avenue, Murray Hill, New Jersey 07974*

<sup>2</sup>*Physics Department, Seoul National University, Seoul, 151-742, Korea*

<sup>3</sup>*Physics Department, University of Michigan, Ann Arbor, Michigan 48109*

<sup>4</sup>*Physics Department, Tohoku University, Sendai 980, Japan*

<sup>5</sup>*Physics Department, Ohio State University, Columbus, Ohio 43210*

(Received 29 March 1993)

We report the observation of a strong temperature dependence of the Kondo resonance in the valence-band photoemission spectrum and of the  $3d \rightarrow 4f$  white line in the x-ray absorption spectrum of  $\text{YbAl}_3$ . The asymmetric Kondo resonance has a binding energy of  $\sim 35$  meV with a  $\sim 50$  meV width. The temperature dependence of the Yb  $4f$  spectral features and valence are well reproduced by Anderson impurity calculations with a Kondo temperature of  $T_K \approx 400$  K, demonstrating that both spectroscopic and near ground state properties can be described within a unified theoretical framework.

PACS numbers: 71.28.+d, 75.20.Hr, 78.70.Dm, 79.60.Bm

In the last decade the Anderson impurity Hamiltonian has been applied to narrow band cerium materials to provide a unified description [1-4] of the Ce  $4f$  spectra, measured with photoemission and inverse photoemission spectroscopies (PES and IPES), and the (near) ground state thermal and magnetic properties associated with Kondo behavior. Central to the description is the occurrence of the sharp Kondo resonance feature near the Fermi energy ( $E_F$ ) in the  $4f$  spectrum. Recently, Joyce, Arko, Lawrence (JAL), and co-workers [5] disputed the unified picture, reporting that in their resonant PES study of a number of Ce materials the near  $E_F$  peak has not only an energy position and width inconsistent with the Kondo temperature  $T_K$ , but also insufficient temperature dependence to justify the use of the Anderson impurity Hamiltonian. For Ce materials, the controversy largely involves complications arising because most of the Kondo resonance intensity is in the IPES spectrum [6,7]. Yb materials provide a much better test case because the Kondo resonance occurs dominantly in the PES spectrum, which can be measured with much better resolution than the IPES spectrum. However, also in a number of these Yb Kondo systems, JAL [8] claim that the near  $E_F$  peak has no temperature dependence and an energy width and position that are inconsistent with the Kondo temperature, thereby casting more doubt on the validity of the Anderson impurity model. Although they state that they accept the Kondo picture for ground state properties, and question only the electron spectroscopy aspects, it is important to realize that the issue is far more serious than that because, as we explain near the end of the paper, it is logically inconsistent to accept a Kondo picture for the bulk ground state properties if the photoemission spectrum of the bulk Yb atoms shows no temperature dependence.

In this paper we report temperature dependent, high-resolution valence-band PES and  $3d \rightarrow 4f$  x-ray absorption (XAS) experiments on  $\text{YbAl}_3$ , a Kondo system with

a Kondo temperature of  $T_K \approx 400$  K [9,10]. We have previously reported preliminary results in which spectra at several different temperatures between 10 and 300 K display a peak near  $E_F$  which is very sharp and has a strong temperature dependence [11,12]. Here we present the results of a complete and systematic study addressing most of the issues raised by JAL [13], including the XAS data and a detailed and very successful analysis of the spectral line shapes using Anderson impurity model calculations in the noncrossing approximation (NCA) [3]. We thereby establish the direct relationship between spectral features and near ground state properties.

The experiments were performed at the AT&T Bell Laboratories Dragon beamline at the National Synchrotron Light Source. Valence-band PES spectra were taken at photon energy  $h\nu = 102$  eV, and the combined photon and electron kinetic energy resolution was 75 meV for the broad scans and 45 meV for the narrow scans. The Fermi level position and the combined energy resolution were determined using a Pt reference. Yb  $3d \rightarrow 4f$  XAS spectra were recorded in the total electron yield mode with a photon energy resolution of  $\sim 3$  eV. Several polycrystalline  $\text{YbAl}_3$  samples were used. The samples were scraped *in situ* at 300 K with a diamond file, exposing a clean area of  $\sim 10 \times 4$  mm<sup>2</sup>, of which  $\sim 8 \times 2$  mm<sup>2</sup> was illuminated. Each time the sample temperature was changed, the position of the sample with respect to the photon beam and electron analyzer was carefully adjusted to compensate for the thermal expansion or contraction of the He cryostat manipulator. The base pressure of the vacuum chamber is  $10^{-10}$  torr.

Figure 1 shows the valence-band PES spectra of  $\text{YbAl}_3$  at 300, 200, 100, and 10 K. The spectra consist of two sets of Yb  $4f$  spin-orbit split features, the narrower of which originates from Yb atoms in the bulk and the broader from divalent Yb surface atoms [14]. The Al  $3s, p$  spectral contribution can be neglected due to the much smaller photoionization cross section. With Yb

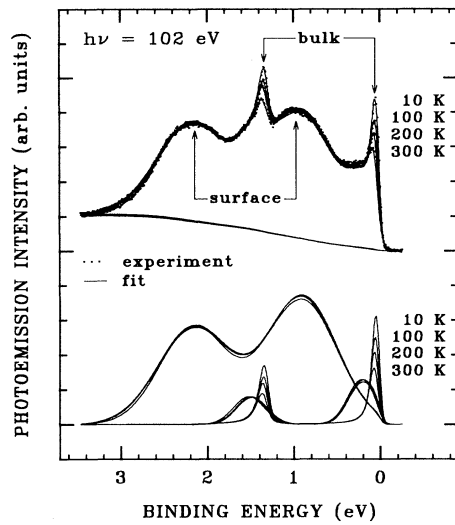


FIG. 1. Temperature dependent valence band PES spectra of  $\text{YbAl}_3$ . Dots are data points, and solid lines are fits as explained in the text.

atoms in the bulk having a nonintegral valence, i.e., fluctuating between two and three, the spectra show that the  $4f^{14}$  configuration must be present in the ground state because the  $4f_{7/2}^3$  and  $4f_{5/2}^3$  PES final states are reached. In contrast to JAL [8], we observe a strong increase of the bulk  $4f_{7/2}^3$  and  $4f_{5/2}^3$  PES intensity when the temperature is lowered from 300 to 10 K, indicating a decrease of the bulk Yb valence. No spectral changes are visible for the surface features. The spectra have been normalized to the photon flux, and a normalization to the Al  $2p$  core-level intensity yields equivalent results [15]. The sample has been scraped at 300 K and the spectra are taken starting with the sample at 300 K and, subsequently at lower temperatures, without rescraping the sample. Using this procedure we have excluded concerns [13] that the observed temperature dependence is due to diffusion of impurities from the bulk, because such diffusion is expected to be already stabilized at 300 K and certainly would not increase with lower temperatures. Also degassing of the cryostat manipulator [13], which might occur if the spectra were taken from low to high temperatures, is prevented. Moreover, any surface contamination that might occur during the cooling down of the sample, is not expected to increase the intensity of very sharp spectral features (with all the  $4f_{7/2}^3$  and  $4f_{5/2}^3$  characteristics for bulk  $\text{YbAl}_3$ ). To further exclude possible artificial temperature effects [13], we have verified repeatedly using several different samples and sample surfaces that the bulk  $4f_{7/2}^3$  intensity is always larger at 77 than at 300 K, no matter how the photon beam is positioned on the sample, and no matter whether the data are taken on warming up or cooling down of the sample.

High resolution PES spectra of  $\text{YbAl}_3$  near  $E_F$  are presented in Fig. 2. A considerable increase of the  $4f_{7/2}^3$  bulk Yb peak intensity can be observed when the temper-

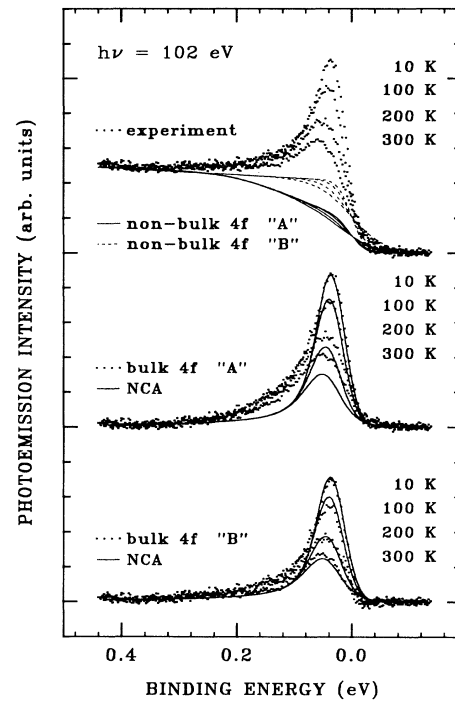


FIG. 2. High resolution temperature dependent valence band PES spectra of  $\text{YbAl}_3$ . Upper panel shows raw experimental data (dots) together with two sets of estimates for the nonbulk  $4f$  spectral contributions, described in the text as "A" and "B." The middle and lower panels show a comparison of the (experimental resolution broadened) NCA results with the bulk Yb  $4f_{7/2}^3$  spectra (dots), obtained after subtracting the respective nonbulk  $4f$  contributions from the raw data.

ature is lowered from 300 to 10 K, and the apparent peak position shifts from  $\sim 55$  to  $\sim 35$  meV binding energy. The FWHM (full width at half maximum) of the asymmetric peak at 10 K is  $\sim 70$  meV, of which  $\sim 50$  meV is intrinsic and 45 meV from experimental resolution. The energy scale of both the position and width of the peak at low temperatures is comparable to the Kondo temperature of  $T_K \approx 400$  K as determined by neutron and susceptibility experiments [9,10], justifying the identification of the peak as the Kondo resonance.

Figure 3 shows Yb  $3d \rightarrow 4f$  XAS spectra at 300 and 10 K, together with the Al  $1s \rightarrow 3p$  edge. The strong Yb XAS indicates an open Yb  $4f$  shell in the ground state of bulk of  $\text{YbAl}_3$ . It is important to note that not only is the XAS more bulk sensitive than the PES, because of the larger probing depth, but also that only the bulk Yb atoms contribute to the XAS signal as the divalent surface Yb atoms have a closed  $4f$  shell configuration. The absence of multiplet,  $3d_{5/2,3/2}$  spin-orbit and satellite structures in the spectra indicate that the XAS is due to the dipole allowed  $3d^{10}4f_{7/2}^1 \rightarrow 3d_{3/2}^2 4f^{14}$  transition, i.e., that the holes in the ground state are primarily of  $4f_{7/2}^3$  character. The Yb XAS intensity decreases by  $11\% \pm 3\%$  when the temperature is lowered from 300 to 10

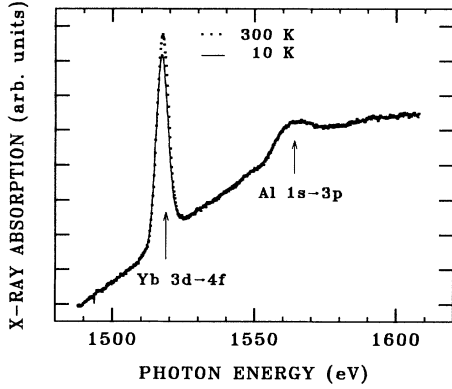


FIG. 3. Temperature dependent  $3d \rightarrow 4f$  XAS spectra of  $\text{YbAl}_3$ , together with the  $\text{Al } 1s \rightarrow 3p$  edge.

K, suggesting that the Yb valence also decreases, consistent with the PES observations.

To quantitatively interrelate the XAS and PES data, we start with an Anderson impurity Hamiltonian, and model the initial state as a linear combination of  $4f^{14}$  and  $4f^{13/2}$  configurations with weights of  $1 - n_f(T)$  and  $n_f(T)$ , respectively. Here  $n_f(T)$  denotes the temperature dependent  $4f$  hole occupancy and the Yb valence is given by  $2 + n_f(T)$ . The two PES final states are  $4f^{13/2,5/2}$  and  $4f^{12}$ , and have negligible hybridization because of their large energy separation, i.e., the  $4f^{13/2,5/2}$  states are at less than 1.5 eV binding energy (see Figs. 1 and 2) and the  $4f^{12}$  multiplets are between 5 and 11 eV binding energy [14]. The PES intensities are then proportional to  $14[1 - n_f(T)]$  and  $13n_f(T)$ , respectively, and the  $3d_{3/2}^9 4f^{14}$  XAS intensity to  $n_f(T)$ .

The hole occupancy  $n_f(T)$  can be determined in various ways. In a recent temperature independent study [14], a value of  $n_f(15 \text{ K}) = 0.65$  has been deduced from the ratio of the  $4f^{13/2,5/2}$  and  $4f^{12}$  PES intensities. In this paper we use the temperature dependence of the spectral features to determine  $n_f$ . With the notation  $\text{PES}(T)$  as the  $4f^{13/2,5/2}$  PES intensity and  $\text{XAS}(T)$  as the  $3d_{3/2}^9 4f^{14}$  XAS intensity at temperature  $T$ , we find from  $\text{PES}(T)/\text{PES}(T_0) = [1 - n_f(T)]/[1 - n_f(T_0)]$  and  $\text{XAS}(T)/\text{XAS}(T_0) = n_f(T)/n_f(T_0)$  that

$$n_f(T_0) = \frac{1 - \text{PES}(T)/\text{PES}(T_0)}{\text{XAS}(T)/\text{XAS}(T_0) - \text{PES}(T)/\text{PES}(T_0)}$$

Figure 4 relates  $\text{XAS}(T)/\text{XAS}(T_0)$  to  $\text{PES}(T)/\text{PES}(T_0)$  for different values of  $n_f(T_0)$ .

To extract  $\text{PES}(300 \text{ K})/\text{PES}(10 \text{ K})$  from the PES data, one has to isolate the spectral contribution of the bulk. In Fig. 1 we roughly approximate the broad non-bulk part by two pairs of spin-orbit split Gaussian line shapes and the sharp bulk part by one pair of spin-orbit split asymmetric Lorentzian line shapes, and include an integral type inelastic background as well. Of the non-bulk emission, the large pair is a known surface feature

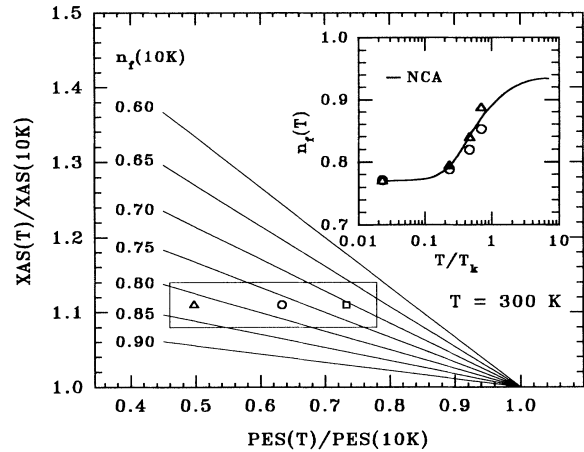


FIG. 4. Determination of the Yb  $4f$  hole occupation number,  $n_f(T)$ , from the temperature dependence of the bulk Yb  $4f^{13/2}$  PES and  $3d \rightarrow 4f$  XAS intensities (see text). The bulk PES intensity is estimated using type "A" (circle) or "B" (triangle) nonbulk  $4f$  correction (see Fig. 2), or assuming a Doniach-Šunjić line shape (square, see text). Inset: Comparison of  $n_f(T)$  from NCA calculations and from experimental bulk Yb  $4f^{13/2}$  PES intensities, using  $n_f(0) = 0.77$ .

[14], and we note that the smaller, temperature invariant pair is like that observed in the high  $T_K$  material  $\text{YbAl}_2$  [15], an impurity phase which is difficult to exclude entirely in  $\text{YbAl}_3$  polycrystals. From the fits to the experimental data we find  $\text{PES}(300 \text{ K})/\text{PES}(10 \text{ K}) = 0.63$ , and together with the XAS data,  $n_f(10 \text{ K}) = 0.77$ . The non-bulk  $4f$  contributions including the temperature dependent Fermi functions are replotted in the upper panel of Fig. 2, where they are labeled as "A," and the resulting pure bulk  $4f$  PES spectra are shown in the middle panel. To do a sensitivity analysis for our bulk/nonbulk separation procedure, we also model the nonbulk  $4f$  contributions simply by linear lines multiplied by the temperature dependent Fermi functions, labeled "B" in the upper panel of Fig. 2, thereby obtaining pure bulk  $4f$  PES spectra as shown in the lower panel, and arrive at  $\text{PES}(300 \text{ K})/\text{PES}(10 \text{ K}) = 0.50$  and  $n_f(10 \text{ K}) = 0.82$ . As yet a third alternative, using Doniach-Šunjić line shapes for the bulk part and Gaussian line shapes for the surface contributions (not shown in this paper), we obtain  $\text{PES}(300 \text{ K})/\text{PES}(10 \text{ K}) = 0.73$  and  $n_f(10 \text{ K}) = 0.71$ , an  $n_f$  value close to that obtained by the temperature independent study [14] which also assumes Doniach-Šunjić line shapes for the bulk features. These  $\text{PES}(300 \text{ K})/\text{PES}(10 \text{ K})$  values are plotted in Fig. 4 against the  $\text{XAS}(300 \text{ K})/\text{XAS}(10 \text{ K})$  value, with the box indicating the margin of error. From this sensitivity analysis we estimate  $n_f(10 \text{ K}) = 0.77 \pm 0.1$ . Defining  $T_K$  by the relation  $\chi(0) = Cn_f(0)/T_K$  [16], where  $\chi(0) = 4.62 \times 10^{-3}$  emu/mol [10] is the experimental static magnetic susceptibility at  $T = 0 \text{ K}$  and  $C = 2.58$  emu K/mol is the Curie constant for the  $j = \frac{7}{2}$   $\text{Yb}^{3+}$  state, and using  $n_f(10 \text{ K})$

for  $n_f(0)$ , we arrive at  $T_K = 430 \pm 60$  K ( $37 \pm 5$  meV) which is in excellent agreement with both the 35 meV binding energy of the Kondo resonance in the low temperature PES spectrum of Fig. 2 and the  $T_K \approx 400$  K from neutron scattering experiments [9].

We have also compared our data with temperature dependent PES spectra calculated using the NCA [3]. The middle and lower panels of Fig. 2 show the results for which a  $4f$  on-site energy of  $\varepsilon_f(j = \frac{7}{2}) = 0.69$  eV and a  $4f$  conduction band hybridization strength of  $\Delta = 57$  meV are used, giving  $n_f(0) = 0.77$  and  $T_K = 410$  K (35 meV). There is good agreement with the experimental pure bulk  $4f$  spectra, although the details depend on the choice for the nonbulk  $4f$  contribution used to correct the raw spectra. Not only is the decrease of the spectral weight with increasing temperature well reproduced, but also the asymmetric line shape and the increase in peak position binding energy with temperature, i.e., from  $\sim 35$  meV at 10 K to  $\sim 55$  meV at 300 K. It is important to note that this decrease of spectral weight and shift to higher binding energies with higher temperature occur not only for the  $4f_{7/2}^{13/2}$  PES peak but also for the  $4f_{5/2}^{13/2}$  peak, both experimentally and theoretically. This gives further support to the notion that the electronic structure of  $\text{YbAl}_3$  must be treated in a many-body framework: In a one-particle picture, one might envision decreasing the  $4f_{7/2}^{13/2}$  peak intensity and increasing the  $4f$  valence by *multiplying* the  $4f$  density of states (DOS) with a thermally broader Fermi function and/or moving the  $4f$  DOS to the unoccupied side of the Fermi level, but such a procedure will not reproduce the behavior of the  $4f_{5/2}^{13/2}$  peak, which lies far from the Fermi level. Finally, Fig. 4 (inset) compares the temperature dependence of the  $4f$  hole occupation  $n_f(T)$ , obtained experimentally from the  $4f_{7/2}^{13/2}$  PES intensity using  $n_f(0) = 0.77$ , and theoretically from the NCA calculations. The good agreement between theory and experiment suggests strongly that changes in the Yb  $4f$  valence with temperature originate from the system spin degrees of freedom. The Kondo singlet state, which is lowest in energy due to mixing of the singlet  $f^{14}$  with the nonmagnetic  $f^{13}$  states, is primarily occupied at low temperatures. The magnetic  $f^{13}$  states, higher lying because they do not mix with the singlet  $f^{14}$ , are increasingly occupied at higher temperatures, driving the valence towards  $3+$ . If the valence were found to be temperature independent, as would be implied by temperature independent bulk  $4f$  PES (or  $3d$  XAS) spectra, the Kondo interpretation of the low energy properties of the bulk could not be maintained. Thus this aspect of  $4f$  PES is intimately linked to the ground state properties and the two cannot be decoupled as JAL [8] seek to do.

To conclude, we have observed a strong and reproducible temperature dependence of the Kondo resonance in the valence band PES spectrum and of the  $3d \rightarrow 4f$  white line in the XAS spectrum of  $\text{YbAl}_3$ . The temperature

dependence of the Yb  $4f$  valence as well as the temperature dependent line shape, position, and intensity of the Kondo resonance, are well reproduced by Anderson impurity model calculations for a system with a Kondo temperature of  $T_K \approx 400$  K, a value obtained from neutron and susceptibility experiments [9,10]. The results strongly support the notion that both electron spectroscopic and near ground state properties can be described within a unified theoretical framework.

It is a great pleasure to acknowledge discussions with O. Gunnarsson, and the technical assistance of G. Meigs and E. E. Chaban. One of us (L.H.T.) would like to acknowledge A. J. Arko, J. J. Joyce, J. M. Lawrence, and R. I. R. Blyth for stimulating discussions and valuable experimental suggestions. Support was provided by the U.S. Department of Energy, Contracts No. DE-AC02-76CH00016 (NSLS), No. DE-FG02-90ER45416 (UM), and No. DE-FG02-87ER45326 (OSU), and by the National Science Foundation, Grant No. DMR-91-08015 (UM).

---

\*Present address: Physics Department, University of Michigan, Ann Arbor, MI 48109.

- [1] J. W. Allen *et al.*, *Adv. Phys.* **35**, 275 (1986).
- [2] O. Gunnarsson and K. Schönhammer, *Phys. Rev. B* **28**, 4315 (1983).
- [3] N. E. Bickers, D. L. Cox, and J. W. Wilkins, *Phys. Rev. B* **36**, 2036 (1987).
- [4] F. Patthey *et al.*, *Phys. Rev. Lett.* **58**, 2810 (1987).
- [5] J. J. Joyce *et al.*, *Phys. Rev. Lett.* **68**, 236 (1992).
- [6] J. W. Allen and O. Gunnarsson, *Phys. Rev. Lett.* **70**, 1180 (1993).
- [7] D. Malterre *et al.*, *Phys. Rev. Lett.* **68**, 2656 (1992).
- [8] J. M. Lawrence *et al.*, *J. Magn. Magn. Mater.* **108**, 215 (1992); J. J. Joyce *et al.*, *Physica (Amsterdam) B* (to be published).
- [9] U. Walter, E. Holland-Moritz, and Z. Fisk, *Phys. Rev. B* **43**, 320 (1991).
- [10] J. C. P. Klaasse, F. R. DeBoer, and P. F. De Châtel, *Physica (Amsterdam)* **106B+C**, 178 (1981).
- [11] S.-J. Oh, *Physica (Amsterdam) B* (to be published).
- [12] More recently, similar data has been obtained by P. Weibel *et al.* (to be published).
- [13] J. J. Joyce, A. J. Arko, and J. M. Lawrence (private communication).
- [14] S.-J. Oh *et al.*, *Phys. Rev. B* **37**, 2861 (1988); E.-J. Cho *et al.*, *Physica (Amsterdam) B* (to be published).
- [15] Using an  $\text{YbAl}_2$  sample and a sample consisting of a mixture of  $\text{YbAl}_2$  and  $\text{YbAl}_3$ , we have verified that the photon flux and Al  $2p$  core-level normalization procedures consistently yield a temperature dependence for the bulk  $\text{YbAl}_3$  features but not for the  $\text{YbAl}_3$  surface and  $\text{YbAl}_2$  bulk features at 0.24 and 1.54 eV binding energy.
- [16] This analytic relation is valid in the first-order calculation of [2], and is used here as an ansatz to define  $T_K$  more generally. For presently unknown reasons, the equivalent NCA expression lacks the factor  $n_f(0)$ .